THERMALLY STIMULATED INVESTIGATIONS ON DIAMOND X-RAY DETECTORS

D. Tromson*, P. Bergonzo, A. Brambilla, C. Mer and F. Foulon
LETI (CEA - Technologies Avancées)/DEIN/SPE, CEA/Saclay, 91191 Gif-sur-Yvette, France
V.N. Amosov
TRINITI, Division of Physics of Thermonuclear Reactors, Troitsk Moscow reg. 142092 Russia
* dominique.tromson@cea.fr
Fax : (33) 1 69 08 76 79
Tel : (33) 1 69 08 62 60

Abstract

Intrinsic diamond material is increasingly used for the fabrication of radiation detectors. However, the presence of inherent defects has a strong impact on the detector characteristics such as the time dependent stability of the detection signal. In order to draw better insights into this effect, comparative investigations of the X-ray responses with thermally stimulated current (TSC) measurements were carried out on natural diamond detectors. TSC revealed the presence of four peaks or shoulders on natural samples in the 200 to 500 K domain. Three energy levels were identified at about 0.7, 0.71 and 0.95 eV. Time dependent X-ray detector sensitivity was investigated for various initial conditions. The results give evidence of the improvement of the detection properties after having filled traps in the material by X-ray irradiation. The comparison between the X-ray response and the TSC spectra indicate that trapping levels emptied at room temperature appear to significantly affect the performance of radiation detectors.

1. Introduction

Intrinsic diamond exhibits a set of properties including a high electrical breakdown field, high electron and hole mobilities and a short carrier lifetime, that make it a very attractive material for electronic applications. Its radiation hardness, high band gap and high thermal conductivity enable its use for the fabrication of radiation detectors operating under harsh radiation and thermal environments. Intensive investigations were carried out on CVD and natural diamonds and it was recently demonstrated that the fabrication of photons as well as particle detectors is readily available [1-6]. However it has been shown that defects and traps can strongly alter the detection properties of the devices [7-9]. Traps or recombination centres in the material reduce the detector sensitivity and thus limit its detection properties. Further, trapping may result in a charge build up, that can strongly modify the space charge in the material during operation. This leads to the evolution of the detector response with the absorbed dose. Thus, the study of the trapping processes in diamond through a comparative investigation between the observed detection properties and the presence of defects, can bring significant improvement in detector technology.

In this paper, the time dependence of the X-ray response of natural diamond detectors is investigated. In parallel, the study of the electrical traps by thermally stimulated current (TSC) technique is reported. The stability of the detector response was analysed together with the TSC response for a range of initial conditions, in order to probe the influence of the defects on the detection signals. It is shown that the levels activated near room temperature unsignificantly affect the X-ray sensitivity of the detectors, but have a significant influence on the stabilisation time of the current after switching off the X-rays.

2. Experimental procedure

The study was conducted on various monocrystalline II-a type natural diamonds. It could be summarized by the analysis of two samples : SA1 (thickness 280 μm) and A03 (thickness 305 μm). SA1 is an unselected commercially available cristal, and A03 is a high quality II-a type diamond, supplied by the TRINITI institute after a drastic selection according to its electronic properties. The high resistivity of diamond samples allows the elaboration of detection devices where diamond is used as a solid ionisation chamber. Detectors with evaporated gold contacts (area : 9 mm^2, thickness : ≈ 50 nm) on both sides of the samples are fabricated.

The devices were placed on a heating-cooling stage in a vacuum chamber. The temperature was varied in the range 100-550 K using a PID controller. A mica platelet ensured the electrical isolation between the device and the heating-cooling stage. Detector operation was performed by applying a voltage across the thickness of the sample. It was irradiated with X-ray photons produced by Bremsstrahlung effect in a X-ray tube through a semi-transparent MgF_2 2 mm thick window. The X-ray energy distribution is spread from 10 to 45 keV with a maximum centred at about 30 keV.

The time dependence of the X-ray response was studied. X-ray photon interaction within the material creates free carriers in the whole volume of the detector. These carriers drift in the electrical field applied on the device, the resulting signal is a photogenerated current that was measured using a Keitley 6517A electrometer.

TSC measurement procedure was performed on discharged diamond samples after an initial heating step at 550 K. Traps were then filled at low temperature by X-ray irradiation. After the X-ray tube was switch off, a linear rise of the sample temperature induced thermal detrapping. This led to the measurement of a temperature-dependent current, basis of the thermally stimulated investigations.

3. Determination of the trap activation energies using TSC measurements

Figure 1 shows the TSC spectra recorded at an heating rate of 0.2 and 0.5 $K.s^{-1}$ on both SA1 and A03 after 10 min of X-ray irradiation when biased under an 1kV/cm applied field. On sample A03, two main well resolved peaks are observed in the 235-550 K range, namely PE1 and PE2 that are centered at about 257 K and 326 K respectively, as well as a shoulder PE3 at about 360 K. The positions of the peaks are given for a 0.2 $K.s^{-1}$ heating rate. The presence of PE1 is clearly identified and is assumed to be caused by annealing treatments performed on this sample as reported from earlier works [10-11]. The PE2 peak has also been reported in the literature by Bowlt [12] and Gorokhovatsky [13] and has been associated to a level at 0.68 eV, eventhough no assumption was made concerning its origin. On sample SA1, a main structure is also visible : the PE2 peak exhibits a shoulder (PO2) around 300 K. Further a peak PO3 can be observed at a slightly higher position than PE3 with a more significant amplitude that was observed for PE3 on sample A03. A shoulder in the PE1 region can also be observed in SA1, eventhough it has not been annealed.

In order to determine the energy levels of the trapping centres, several methods can be used from the analysis of the TSC spectra [14]. The initial rise method [15] assumes that the TSC current is proportional to $\exp(-E_t/kT)$ when the traps begin to be emptied. The energy E_t of traps can be calculated from the slope of the straight line on an Arrhenius plot. This method is independent of the kinetics involved in the process but is applicable only up to 5% of the maximum intensity of the peaks, which prevents its use in the present study because of the extremely low peak intensities. Using the various heating rate method, the energy of trapping levels can be determined using two different heating rates β_1 and β_2. The corresponding maximum temperatures of the TSC spectra T_{m1} and T_{m2} are then determined from the TSC spectra and the activation energy is then given by :

$$E = \left(\frac{kT_{m1}T_{m2}}{T_{m1} - T_{m2}} \right) Ln \left(\frac{\beta_1 T_{m2}^{\ 2}}{\beta_2 T_{m1}^{\ 2}} \right) \quad (1)$$

As shown by Hoogenstraaten [16] the use of several heating rates yields to the activation energy of a level with a good accuracy for the first order kinetics whereas very good approximation is obtained for the general order kinetics. This method gives accurate results when the TSC peaks are well resolved. If peaks are overlapping, the measured value of the maximum temperature T_m can be substantially influenced by the neighbouring peaks resulting in misleading energy values. In this case, a computerised deconvolution method can be used, namely the MINUIT code developed at CERN [17] that was applied in this study for the deconvolution of well resolved peaks following a first or a general order kinetics. The results of the fits are shown on figure 2 for sample A03. Table 1 gives the resulting activation energy of traps using the heating rate methods and the numerical analysis. On sample A03 both methods were well adapted because of the good resolution on PE1 and PE2. However, since the various heating rate method depends on the visual appreciation of the peak position, significant differences in the value of the calculated energy levels may result. On sample SA1, because of the bad resolution of the peaks, the deconvolution analysis and heating rate method were not so well adapted to the determination of the energy level : the calculation was restricted to PE3, eventhough the presence of the shoulder in the low region of this peaks may induce an error on the calculated value.

4. Response under X-ray flux

Figure 3 shows the X-ray responses of both samples as a function of time at room temperature. The response of the detectors were recorded at a dose rate of about 8 Gy/h under an applied field of 1 kV/cm. After approximately two minutes of irradiation, sample A03 exhibits a stable current response with respect to the duration of the experiment. On the opposite, a significant evolution of the recorded signal is observed on sample SA1, since the photogenerated current has not reached a stable value after 30 mn. The current levels observed in SA1 also remain below those observed in A03. This evolution is highly detrimental for the fabrication of radiation detection devices. Losses in the signal recorded may be caused by the interaction of the generated carriers with traps and recombination centres. If part of the carriers, created by the X-ray irradiation, are trapped in the bulk, the amount of the induced charge at the detector output remains lower than the generated charge, and the collection efficiency (i.e the ratio of the induced charge by the generated charge) of the detector is reduced. If we assume that the sample has reached a stable state, the lower current levels observed could be caused by the loss of part of the generated carriers. Further, the evolution of the detection signal with time could be explained by the progressive evolution of the trap filling mechanism. Also, the presence of charge trapping may induce a modification of the space charge in the material with the duration of the experiment which could result in the evolution of the effective applied field on the material and therefore modify the detector response. When the traps are filled in a new equilibrium state, the collection efficiency remains stable. Similar effects reported as priming or pumping effects and caused by the passivation of traps are known to improve the value of the collection efficiency [18].

Looking at the kinetics of the X-ray response, figure 3 also shows that the shape of the X-ray response exhibits varying inflexion during the irradiation time. Under the assumption that the trap filling procedure is responsible for the evolution of the X-ray sensitivity, this could be explained by the presence of traps which are more active at room temperature on sample SA1 than on sample A03. The trap filling procedure concerns all levels released above room temperature, and therefore those reported on the TSC spectra, but also other deeper

levels activated at higher temperatures. The stable state is reached when the traps are in a new equilibrium, and when this charged state remains at the operation temperature of the experiment.

Figure 4 shows the responses of SA1 : (i) under successive X-ray irradiations at room temperature, the X-ray tube being switch off for a short period of time, and (ii) under X-ray irrradiations after the sample was left in the dark for 17 hours. It shows that the stable state of the sample reflects the progressive filling of deep traps. Indeed, after having left the sample biased in the dark for a long period of time , the X-ray response measured after a new irradiation reaches the same current level, thus confirming that the levels emptied at or below room temperature are of little influence on the X-ray sensitivity. Nevertheless, a little overshoot is visible after a long waiting time in the dark at room temperature. This could be correlated with the behaviour of the dark current after switching off the X-rays. The slow decrease of the dark current is responsible of a change in the charged state of the sample which could modify the X-ray response of the sample.

5. Comparative study of the X-ray responses with the TSC spectra

In order to study the correlation between the presence of traps and the X-ray responses of the detectors, the X-ray responses and TSC spectra were successively recorded for various durations of the trap filling step (X-ray irradiation) and detrapping step (sample left in the dark after X-ray irradiation and before the TSC measurement). Between each measurement, the samples were annealed at 550 K to return to the initial detrapped state.

The insert in figure 5 shows the X-ray response of the A03 detector during the trap filling steps under X-ray irradiation for 10 s, 1 mn and 5 mn. It appears that the stabilisation time on A03 is very short thus indicating that the first slope in the deviation phenomenon is observed during the first minutes of irradiation. Further, after switching off the X-rays, the turn off time of the diamond is very fast. The corresponding TSC spectra in figure 5 show that the amplitude of the TSC peaks PE2 and PE3 increase with the time of irradiation while the relative amplitudes of these two peaks is maintained. The influence of the duration of the detrapping step on the TSC spectra was also investigated. The TSC spectra recorded 10 s and 10 mn after having stopped the X-ray irradiation showed no variation in the relative amplitudes of the PE2 and PE3 peaks.

In contrast to A03, the response of SA1 to X-rays revealed a long stabilisation time and a slow turn off time of several minutes, as shown in the insert in figure 6 (a) for 10 and 55 mn irradiations. The TSC spectra recorded after the sample was kept at 300 K for a fixed time of 6 mn are given in figure 6. It is clearly visible that the relative amplitudes of the PE2 and PO3 peaks remain constant for the differing durations of irradiation. This shows that the trap filling procedure related to both peaks is proportional to the X-ray exposure time in a similar way to what was observed for the A03 sample. The PO2 shoulder, which was observed on SA1 (see figure 1 (b)) around 300 K, is not seen in the TSC spectra in figure 6 (a). Indeed, these latter spectra were recorded from a starting temperature of 300 K, i.e when the detrapping associated to the PO2 shoulder has already taken place.

Figure 6 (b) shows the TSC spectra recorded after successive trap filling steps of 10 mn (from initial detrapped state) followed by detrapping steps with various durations : 2, 6 and 15 mn. The spectra show significant differences in the relative amplitudes of the PE2 and PO3 peaks. The amplitude of the PE2 peak decreases whereas the amplitude of the PO3 peak remains constant. Further, the position of the PE2 peak in figure 6 (b) shifts to higher temperatures when the detrapping time is increased. This could indicate that the PE2 peak observed on sample SA1 would be the convolution of several peaks with those centred at the

lowest temperatures decreasing in intensity during the detrapping step at room temperature. The discharge of the low temperature part (~ 300 K) of the wide PO2-PE2 structure is most probably responsible for the slow turn off time of the SA1 detector. As such, and as seen on Figure 4, this slow decrease of the dark current at room temperature illustrates a phenomenon of the trapped carriers release from a level activated close to this temperature. On the opposite, on sample A03, the turn off time was very short, and the TSC spectra revealed similar relative amplitudes between the PE2 and PE3 peaks. This tends to attribute the slow turn off times to the presence of the PO2 (as well as to the low temperature part of the PE2 level) which was not apparent on A03.

This is further confirmed on Figure 7 which shows the turn off times of SA1 recorded at 300 and 435 K. The turn off times were recorded after the detector had reached comparable trap filling states, i.e. when the detector current under X-ray irradiation reached 6 x 10^{-11} A. At 435 K, the turn off time is very short in comparison with that at 300 K. Thus, no detrapping is observed at 435 K. This confirms that the slow turn off time of SA1 at room temperature is caused by the PO2-PE2 structure while level activated at higher temperatures does not seem to affect the detector turn off time at room temperature [19].

6. Summary

Thermally stimulated current measurements were carried out in parallel with a study on the time dependent evolution of the X-ray response of natural diamond detectors. From the TSC spectra, three energy levels were determined at 0.7, 0.71 and 0.95 eV. They correspond to TSC peaks centred at about 257, 326 and 360 K. X-ray responses showed that the time stability of the signal after turn-on and turn-off was strongly sample dependent. The study demonstrated that the X-ray sensitivity is little affected by levels emptied at or below room temperature. In contrast, these levels seem to have a significant influence on the stabilisation time of the current after the X-rays are switched off. In particular, structures identified here as PO2-PE2, and PO3 released around room temperature, appear to be responsible of the slow decay of the signal in randomly purchased II-a type stones. It is shown that highly selected II-a type diamond, does not exhibit the same TSC characteristics in this region, nor the slow signal decay signature. Since no data is currently available, further characterisation is needed in order to identify the nature of these defects which can be extremely detrimental for the fabrication of radiation detectors.

References

[1] P. Bergonzo, F. Foulon, R. D. Marshall, C. Jany, A. Brambilla, R. D McKeag, R. B. Jackman, IEEE Trans. Nucl. Sci. **45**, 370 (1998).

[2] F. Foulon, P. Bergonzo, A. Brambilla, C. Jany, B. Guizard, R. D. Marshall, MRS Proc. **487**, 591 (1998).

[3] F. Foulon, P. Bergonzo, C. Borel, R. D. Marshall, C. Jany, L. Besombes, A. Brambilla,. J. Appl. Phys. **84**, 5531 (1998).

[4] P. Bergonzo, A. Brambilla, D. Tromson, R. D. Marshall, C. Jany, F. Foulon, C. Gauthier, V. A. Sole, J. Goulon, J. Synchrotron Rad. **6**, 1 (1999).

[5] C. Manfredotti, P. Polesello, M. Truccato, E. Vittone, A. Lo Giudice, F. Fizzotti, Nucl. Inst. And Meth. A **410**, 96 (1998).

[6] RD 42 Collaboration, Nucl. Inst. And Meth. A **409**, 264 (1998).

[7] E-K. Souw, R. J. Meilunas, Nucl. Inst. And Meth. A **400**, 69 (1997).

[8] T. Pochet, A. Brambilla, P. Bergonzo, F. Foulon, C. Jany, A. Gicquel, Conference Proceedings Vol.**52**, "Eurodiamond '96", Ed. C. Manfredotti, R. Vittone, p.111 (1996).

[9] S. F. Kozlov, R. Stuck, M. Hage-Ali, P. Siffert, IEEE Trans. Nucl. Sci. **42**, 160 (1975).

[10] D. Tromson, P. Bergonzo, A. Brambilla, C. Mer, F. Foulon, Phys. Stat. Sol. (a) **174**, 155 (1999).

[11] O. Gaudin, S. Watson, S. P. Lansley, H. J. Looi, M. D. Whitfield, R. B. Jackman, Diamond Relat. Mater. **8**, 886 (1999).

[12] C. Bowlt, J. Phys. D: Appl. Phys. **6**, 616 (1973).

[13] Yu. A. Gorokhovatsky, L. V. Grigoriev, V. B. Kvaskhov, A. N. Pitirimov, K. L. Temnikov, Proceedings of the 8th International Symposium on Electrets, 7-9 september 1994.

[14] R. Chen, Y. Kirsh, Analysis of Thermally Stimulated Processes, International Series on the Science of the Solid State, Vol **15** (1981).

[15] G. F. J. Garlick and A. F. Gibson, Proc. Phys. Soc. **60**, 574 (1948).

[16] W. Hoogenstraten, Philips Res. Repts. **13**, 515 (1958).

[17] F. James, M. Roos "MINUIT. A system for function minimization and analysis of the parameters errors and correlation" CERN Computer Center Program Library D-506, (1997).

[18] T. Behnke, A. Oh, A. Wagner, W. Zeuner, A; Bluhm, C-P. Klages, M. Paul, L. Schafer, Diamond Relat. Mater. 7 1553 (1998).

[19] P. Gonon, S. Prawer, Y. Boiko, D.N. Jamieson, Diamond Relat. Mater. **6**, 860 (1997).

Figure captions

Fig. 1. TSC spectra recorded for two heating rates in the 235-550K range on sample A03 (a) and SA1 (b).

Fig. 2. Deconvolution analysis on sample A03. The results give three levels at about 0.7, 0.71 and 0.95 eV for the PE1, PE2 and PE3 respectively.

Fig. 3. Response of A03 and SA1 detectors under X-ray irradiation. On sample SA1 the presence of traps induces an evolution of the signal recorded with the duration of the irradiation.

Fig. 4. X-ray response of sample SA1 after successive irradiations.

Fig. 5. TSC spectra recorded after various durations of irradiation on A03. The insert shows the X ray response of the detector.

Fig. 6. TSC spectra recorded on SA1 for (a) various durations of irradiation, the insert show the corresponding X-ray responses, the sample being kept at room temperature for 6 minutes before measurements, and (b) for the same durations of irradiation, but using different relaxation times between measurements.

Fig. 7. Relaxation currents of sample SA1 at 300K and 435K.

Table. 1. Trap activation energies on A03 using both the deconvolution analysis and the heating rate method

A03	PE1	PE2	PE3
Heating rate method	0.63 eV	0.76 eV	-
Deconvolution analysis	0.7 eV	0.71 eV	0.95 eV

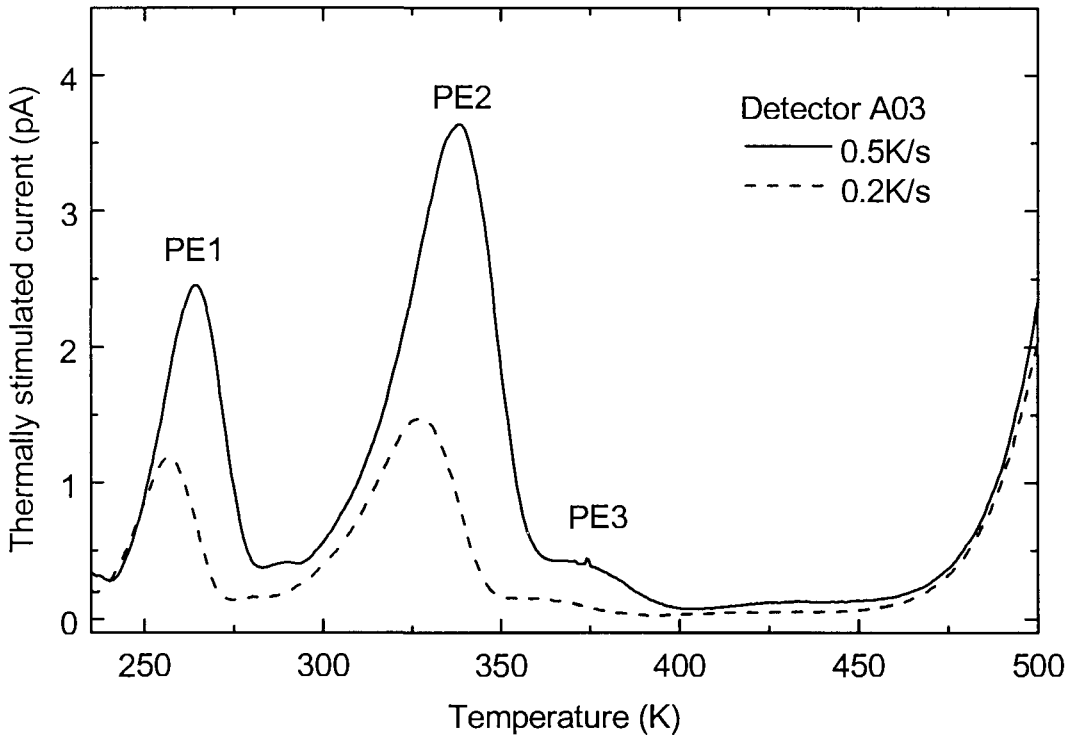
Thermally stimulated current (pA)
Temperature (K)
PE1
PE2
PE3
Detector A03
0.5K/s
0.2K/s
0
1
2
3
4
250
300
350
400
450
500

Fig. 1 (a)

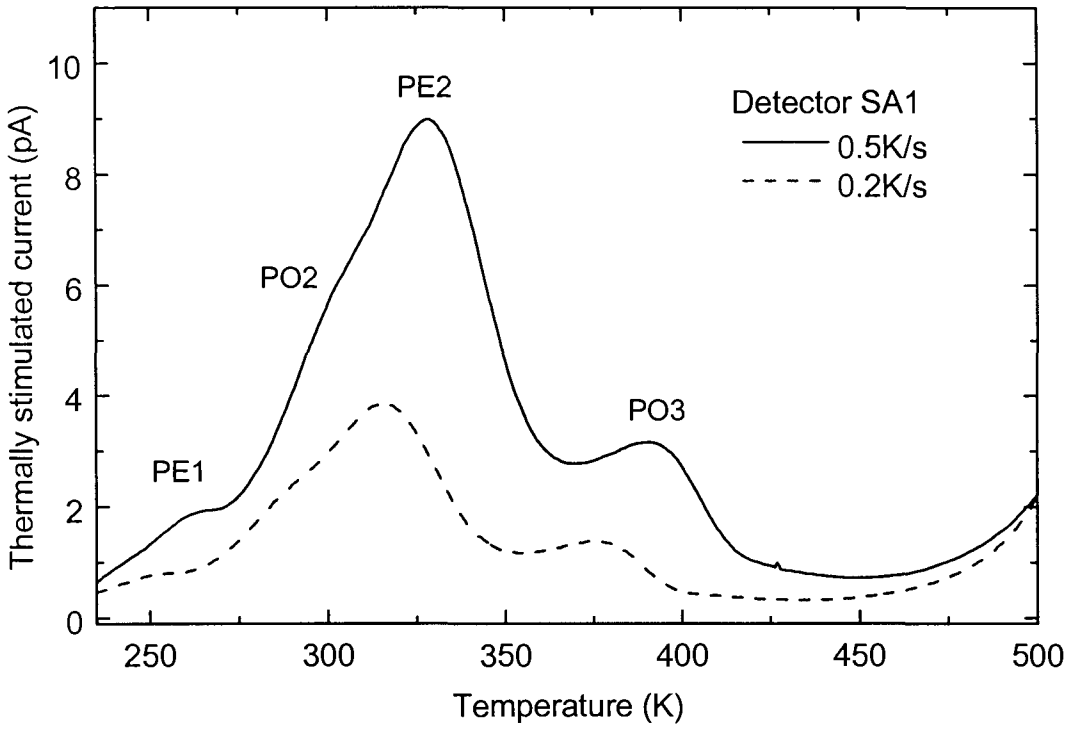
Thermally stimulated current (pA)
Temperature (K)
PE1
PO2
PE2
PO3
Detector SA1
0.5K/s
0.2K/s
0
2
4
6
8
10
250
300
350
400
450
500

Fig. 1 (b)

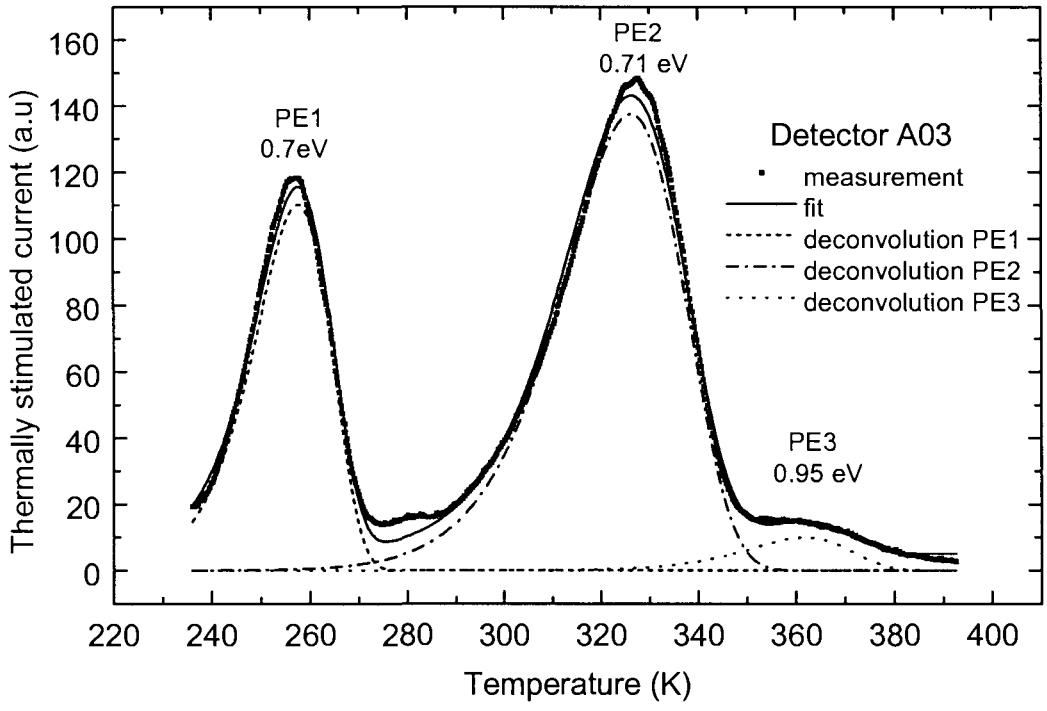
PE1
0.7eV
PE2
0.71 eV
PE3
0.95 eV
Detector A03
measurement
fit
deconvolution PE1
deconvolution PE2
deconvolution PE3
Thermally stimulated current (a.u)
Temperature (K)
0
20
40
60
80
100
120
140
160
220
240
260
280
300
320
340
360
380
400

Fig. 2

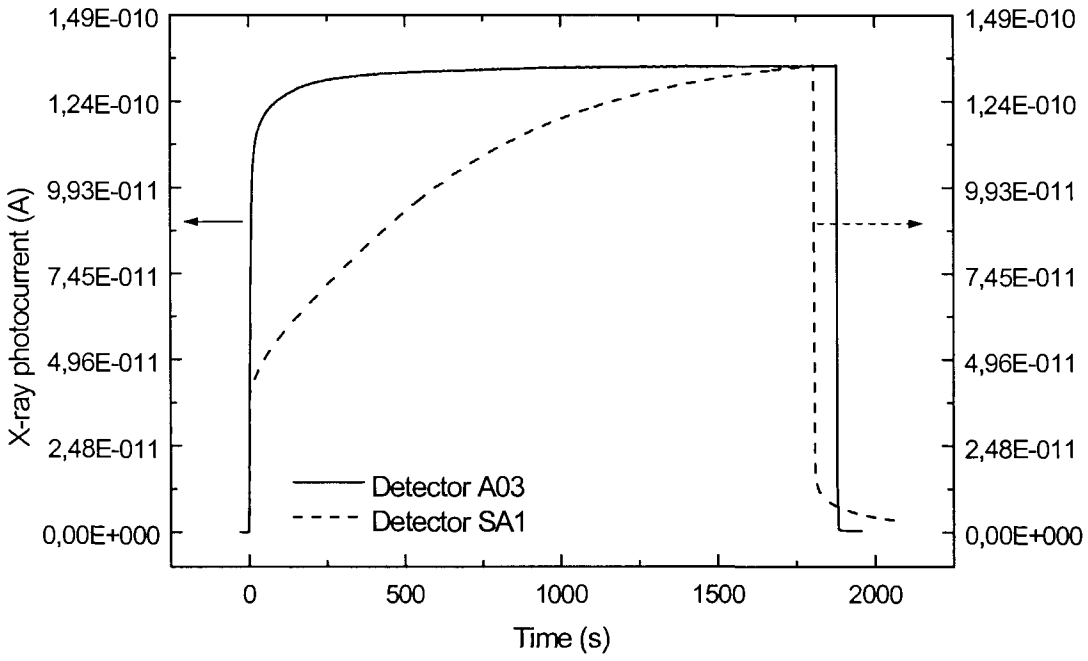
1,49E-010
1,24E-010
9,93E-011
7,45E-011
4,96E-011
2,48E-011
0,00E+000
X-ray photocurrent (A)
Detector A03
Detector SA1
0
500
1000
1500
2000
Time (s)

Fig. 3

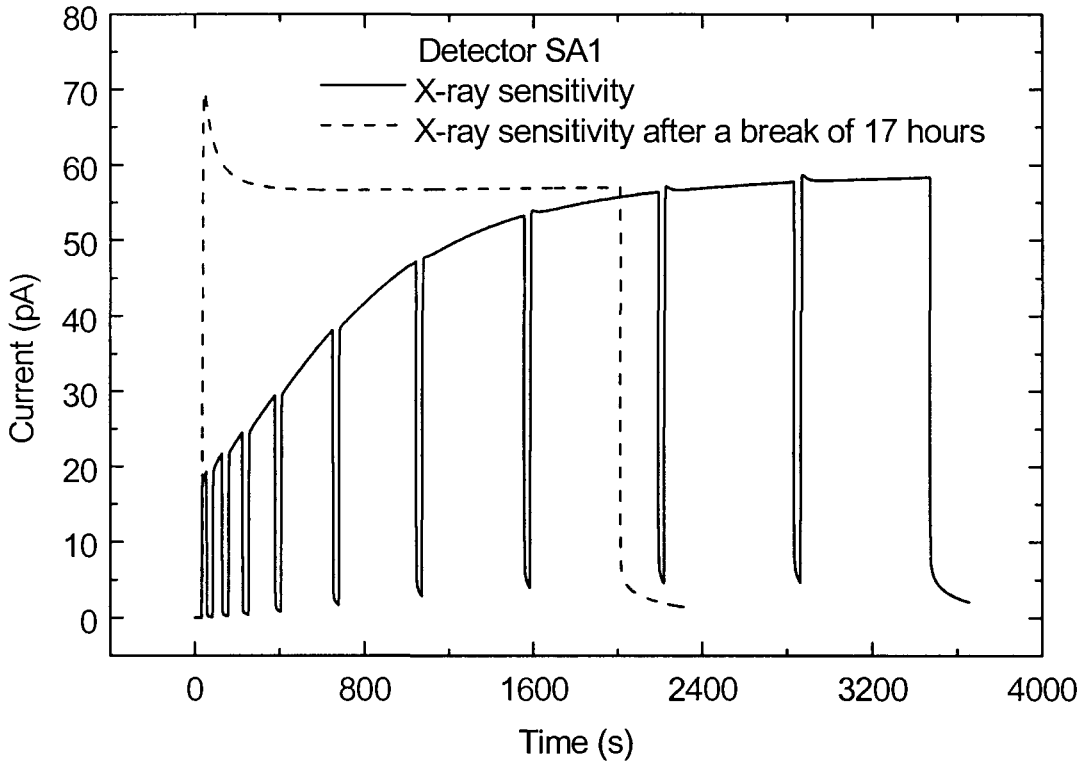
Detector SA1
X-ray sensitivity
X-ray sensitivity after a break of 17 hours
Current (pA)
Time (s)
0
10
20
30
40
50
60
70
80
0
800
1600
2400
3200
4000

Fig. 4

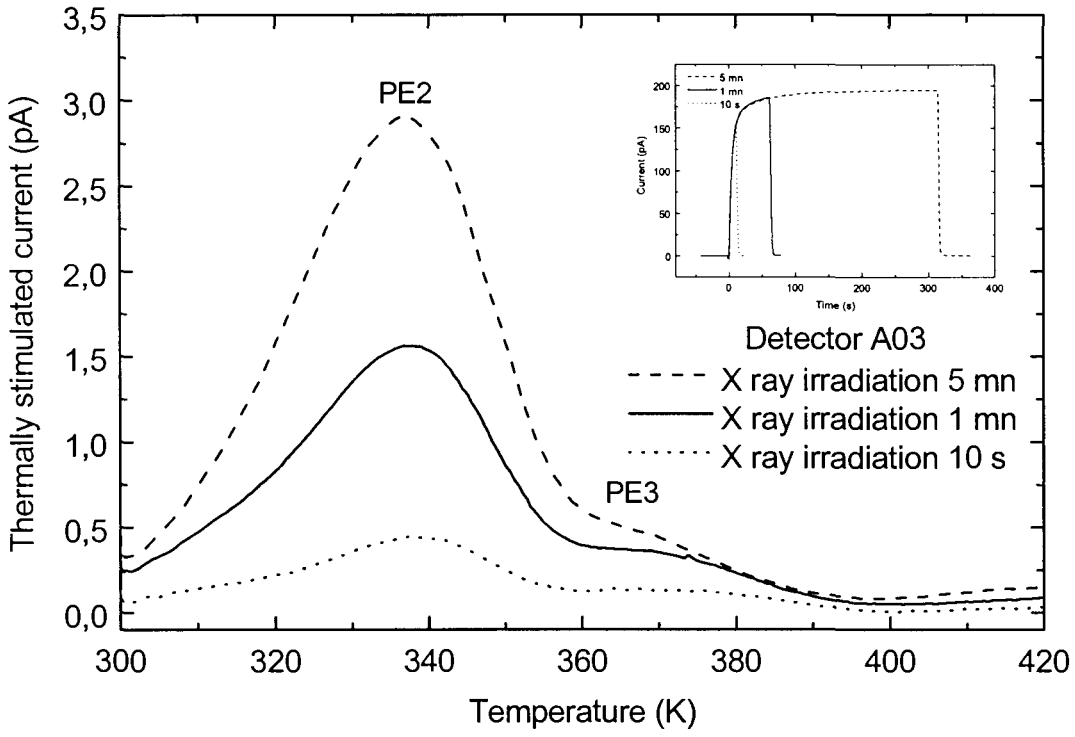
Thermally stimulated current (pA)
Temperature (K)
PE2
PE3
Detector A03
X ray irradiation 5 mn
X ray irradiation 1 mn
X ray irradiation 10 s
5 mn
1 mn
10 s
Current (pA)
Time (s)

Fig. 5

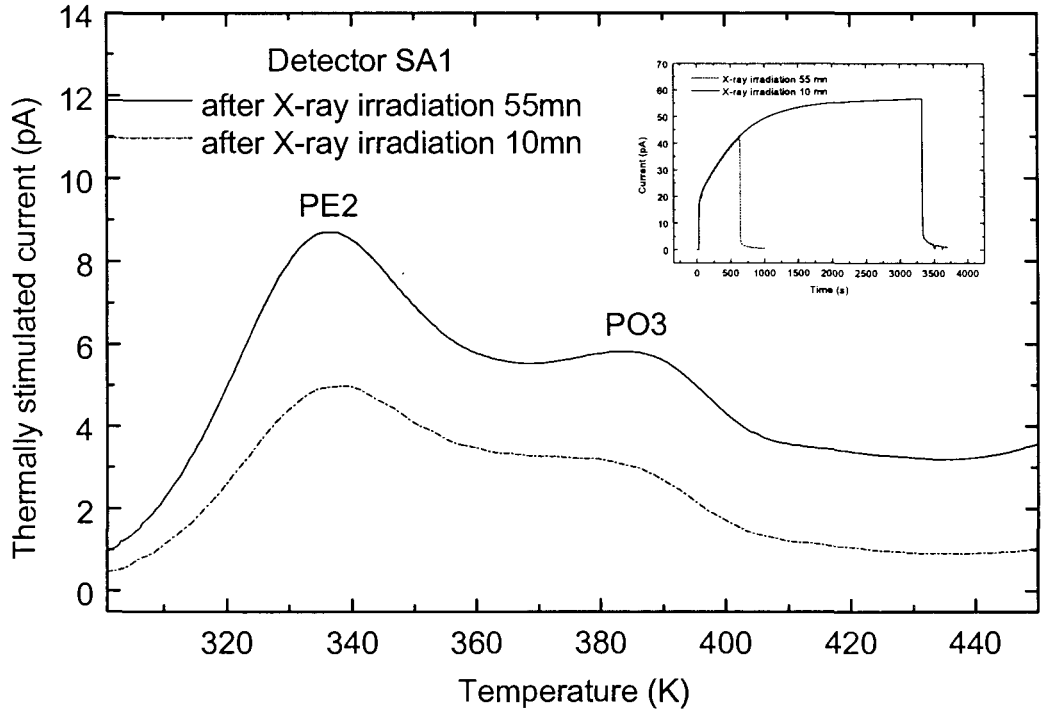
Thermally stimulated current (pA)
Temperature (K)
Detector SA1
after X-ray irradiation 55mn
after X-ray irradiation 10mn
PE2
PO3
X-ray irradiation 55 mn
X-ray irradiation 10 mn
Current (pA)
Time (s)

Fig. 6 (a)

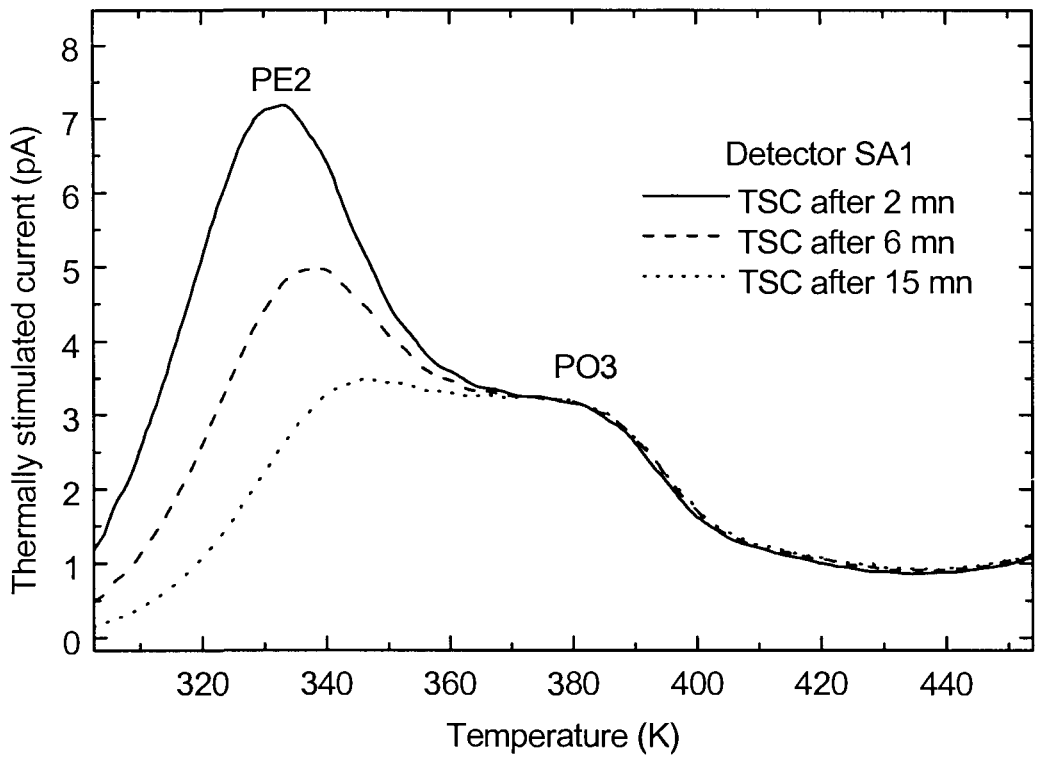
PE2
PO3
Detector SA1
TSC after 2 mn
TSC after 6 mn
TSC after 15 mn
Thermally stimulated current (pA)
Temperature (K)
0
1
2
3
4
5
6
7
8
320
340
360
380
400
420
440

Fig. 6 (b)

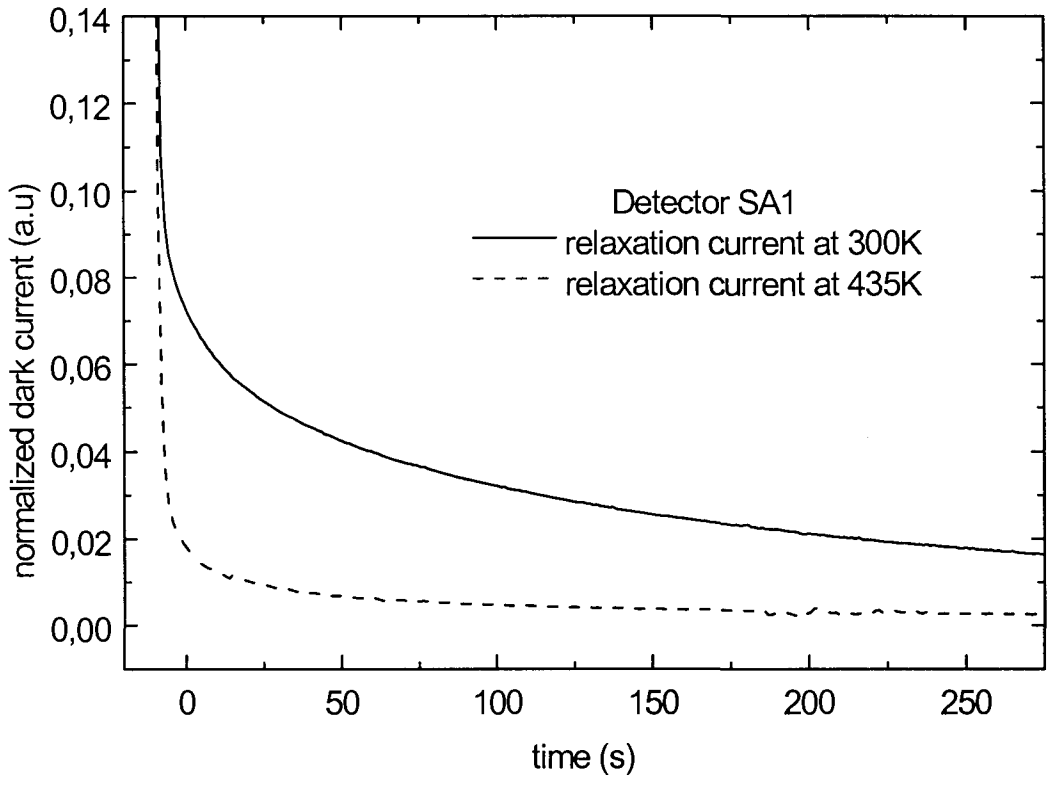
0,14
0,12
0,10
0,08
0,06
0,04
0,02
0,00
normalized dark current (a.u)
0
50
100
150
200
250
time (s)
Detector SA1
relaxation current at 300K
relaxation current at 435K

Fig. 7